ACS SYMPOSIUM SERIES 567

Formulation and Delivery of Proteins and Peptides

Jeffrey L. Cleland, EDITOR
Genentech, Inc.

Robert Langer, EDITOR
Massachusetts Institute of Technology

Developed from a symposium sponsored
by the Division of Biochemical Technology
at the 205th National Meeting
of the American Chemical Society,
Denver, Colorado,
March 28–April 2, 1993

American Chemical Society, Washington, DC 1994

Chapter 15

Drug Delivery from Bioerodible Polymers

Systemic and Intravenous Administration

Achim Göpferich[1,2], Ruxandra Gref[1,3], Yoshiharu Minamitake[1], Lisa Shieh[1], Maria Jose Alonso[1,4], Yashuhiko Tabata[1,5], and Robert Langer[1]

[1]Department of Chemical Engineering, Massachusetts Institute of Technology, Building E25, Room 342, Cambridge, MA 02139
[2]Lehrstuhl für Pharmazeutische Technologie, Universität Erlangen–Nürnberg, Cauerstrasse 4, 91058 Erlangen, Germany
[3]Laboratoire de Chimie Physique Macromoleculaire, Ecole Nationale Supérieure des Industries Chimiques, 1 rue Grandville, 54001 Nancy Cedex, France
[4]Laboratorio de Farmacia Galénica, Facultad de Farmacia, Universidade de Santiago de Compostella, 15706 Santiago de Compostella, Spain
[5]Research Center for Biomedical Engineering, Kyoto University, 53 Kawahara-cho, Shogoin, Sakyo-ku, Kyoto 606, Japan

The recent progress in understanding the erosion of biodegradable polymers and the manufacturing of controlled release devices for proteins and peptides is reported. The erosion mechanism of poly(anhydrides) was investigated as an example of biodegradable polymers and the erosion behavior is modeled mathematically. The results provide useful information on the microstructure and chemical environment inside these polymers during erosion. It is shown how they might affect the stability and the release of proteins. Concomitantly proteins were processed in controlled release devices. Special attention was paid to the stability of the biomolecules during the manufacturing of dosage forms. Furthermore, the development of a new type of biodegradable nanosphere as a future dosage form is shown.

Progress in the field of biology and biochemistry has led to the discovery of numerous bioactive peptides and proteins in the last few decades. Many of them, like insulin, as a classical example, are very useful for medical therapy. The rapid development of biotechnology and progress in peptide and protein chemistry allowed the mass production of many compounds and made their broad introduction into medical therapy possible(*1*). The

0097–6156/94/0567–0242$10.88/0

use of such biomolecules poses, however, severe problems. Some of these compounds have very short half lives in body fluids (under a minute, in some cases(*2*)) and due to degradation in the gastrointestinal tract the majority of them cannot be administered orally. These limitations motivated the development of controlled release dosage forms that improve protein and peptide stability as well as prolong drug activity after application. Processing these substances into dosage forms is not always easily achieved. Many of them have limited chemical and physical stability. Common instabilities are irreversible aggregation(*3*), oxidation(*4*) or conformational changes(*5*) all of which may affect activity. The preparation of controlled release devices for such proteins and peptides has, therefore, become one of the major challenges in the field of controlled release.

Controlled release devices have been prepared for various routes of administration such as oral, parenteral, nasal, rectal, buccal, vaginal and transdermal(*6-7*). They all control the release of peptides and proteins by a few basic principles. Classical systems control release by diffusion through a polymer matrix, in which the drug might be dissolved or suspended(*8*). Closely related to diffusion controlled release systems are those in which swelling controlled release occurs(*9*). The swelling of the polymer, usually an ionic network, increases the permeability of the matrix and allows drugs to be released by diffusion. Parenterally applied dosage forms are the most often used at present as many proteins and peptides are unstable in the gastrointestinal tract resulting in poor bioavailability. The introduction of degradable drug carrier materials brought new progress into this field of controlled release research. Biodegradable polymers as drug carriers control the release of the drugs through diffusion and erosion and have the advantage of dissolving after the application. Instead of simple diffusion-controlled release, drug is release by an erosion-controlled mechanism, which provides the advantage of decreasing the release rate of the proteins and peptides. The search for new biodegradable polymers for controlled release stimulated research in several areas, such as polymer synthesis, polymer processing and the formulation of devices. In the area of polymer synthesis, there have been major efforts to 'design' polymers for the purpose of controlled release. Appropriate examples are poly(ortho esters)(*10*) and poly(anhydrides)(*11*). In providing the biodegradable polymer raw material for controlled release devices for peptides and proteins two fundamental problems arose:

1. In order to efficiently design a controlled release device from biodegradable polymers, the polymer properties and its erosion mechanism should be known.
2. The technology for manufacturing devices ranging from the centimeter to the nanometer scale must be developed. The requirements of stability for such sensitive compounds as peptides and proteins must, thereby, be met.

The successful design of release systems will heavily depend on detailed knowledge in both areas. Unfortunately, a unique theory does not

exist for either set of issues. There is not, for example, a basic theory that could predict the erosion of all biodegradable polymers or the stability of proteins and peptides from their structural formulas alone. Due to the expanded research in these areas, however, there is progress towards a broader understanding of polymeric properties and the development of stable protein formulations compatible manufacturing technology. This article intends to show some of the progress that has been made in understanding the release of peptides and proteins from polymers. The focus will be on two major areas:

1. Understanding the erosion mechanism of biodegradable polymers.
2. Providing some examples to illustrate recent advances in the development of controlled release systems. We cover the release of proteins from polymers as well as the development of future dosage forms.

The Erosion of Biodegradable Polymers

Investigating erosion mechanisms of biodegradable polymers might look rather academic and not that beneficial at first glance. The microenvironment of a biodegradable polymer during erosion, however, provides the medium in which peptides and proteins are embedded and from which they have to be released. Factors like pH or the amount of dissolved monomers not only influence release rates, but also affect the stability of proteins and peptides substantially(*12*) and thus become very important parameters for the stability of a controlled release dosage form. The design of manufacturing systems for the controlled release of proteins and peptides from polymers requires, therefore, a fundamental knowledge the erosion mechanism of a biodegradable polymer.

Diffusion controlled protein release from non-degradable polymers is well-understood(*13*). The release of such compounds from biodegradable polymers in contrast depends heavily on the erosion of the polymer, a complex process whose mechanism is not entirely understood. The erosion of biodegradable polymers follows mechanisms specific for a certain type of polymer and is influenced by a number of parameters. Most important is the chemical *degradation* of bonds in the polymer chain. The rate at which the bonds are cleaved depends on the type of bonds between the monomers(*14*), the diffusivity of water in the polymer(*15*), and the polymer crystallinity(*16*). The pH of the degradation medium exhibits a catalytic effect on the hydrolysis of bonds(*17*), influences the solubility of degradation products, and finally regulates their release. Degradation products such as Monomers and oligomers carry functional groups that change pH inside cracks and pores in the eroded polymer and these groups can have feedback on the erosion process(*18*). It can be concluded that the polymer erosion is a composite process that can be very complex and is specific for each polymer. The erosion mechanisms of poly(lactic-co glycolic acid) and poly(ortho esters), for example, follow completely different mechanisms(*19-20*).

Investigation of Erosion Mechanisms. We were interested in the erosion mechanism of a class of related poly(anhydrides) consisting of sebacic acid (SA), 1,3-bis(p-carboxyphenoxy)propane (CPP) and a fatty acid dimer (FAD) monomers which are shown in Figure 1. The techniques that were used for these studies may be applied to any class of polymer and the results that we obtained provide a clear outline for the important fundamental characteristics of polymer erosion.

The Structure of Polymers. Prior to the investigation of eroded polymer discs, the polymers were investigated for their internal structure. Figure 2 shows the appearance of various polymers that were taken from thin melted polymer films under polarized light. The Maltese Crosses indicate that these polymers are partially crystalline and consist of spherulites. The crystallinity of the polymers depends on the copolymer composition. In the case of poly(1,3,-bis(p-carboxyphenoxy)propane-co-sebacic acid) abbreviated p(CPP-SA) changing the content of either monomer to a 50:50 composition lowers the crystallinity from more than 60% to almost 10% (*21*). Concomitantly, the glass transition temperature drops substantially. p(FAD) homopolymer is amorphous(*22*), so that the crystallinity of p(FAD-SA) copolymers depends only on the SA monomer content. As shown in Figure 3, increasing the content of FAD monomer above 80% results in amorphous polymers. The effect of microstructure and crystallinity on erosion is observed in investigating eroded polymer discs that were produced from the polymer by melt molding(*11*). Figure 4 a shows a scanning electron photograph of a cross section through a disc of p(CPP-SA) 20:80 that has been eroded in phosphate buffer pH 7.4 at 37°C for 3 days. Eroded and non-eroded polymer sharply separated by the erosion front are readily distinguishable. Observation of this front with time confirms that the erosion of these polymers starts on the surface and moves towards the center of the discs which has been referred to as surface erosion(*23*). Figure 5 shows the kinetics of front movement in p(CPP-SA) 20:80 and p(CPP-SA) 50:50 as measured from SEM pictures. The way erosion affects the polymer can be seen from SEM pictures showing the eroded parts of the polymer in more detail. As shown in Figure 4b the amorphous parts of the spherulites have been eroded, while the large parts of the crystalline skeleton remain in place(*24*). As erosion progresses, a highly porous erosion zone is created. Once the erosion front has reached a certain spot in the matrix, the release of drug begins from that point. The release of compounds is then determined by the diffusion through pores and cracks.

pH Changes during Erosion. When these polymers erode, they release oligomers and monomers that carry carboxylic groups (*25*). We suspected that the pH in the vicinity of the polymer surface or inside the cracks and pores of the polymer is not determined by the pH of the buffer medium, but instead by the released monomers. To support this hypothe-

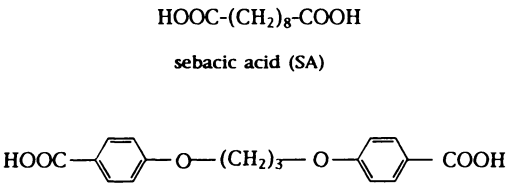

Figure 1. Monomers contained in the investigated poly(anhydrides).

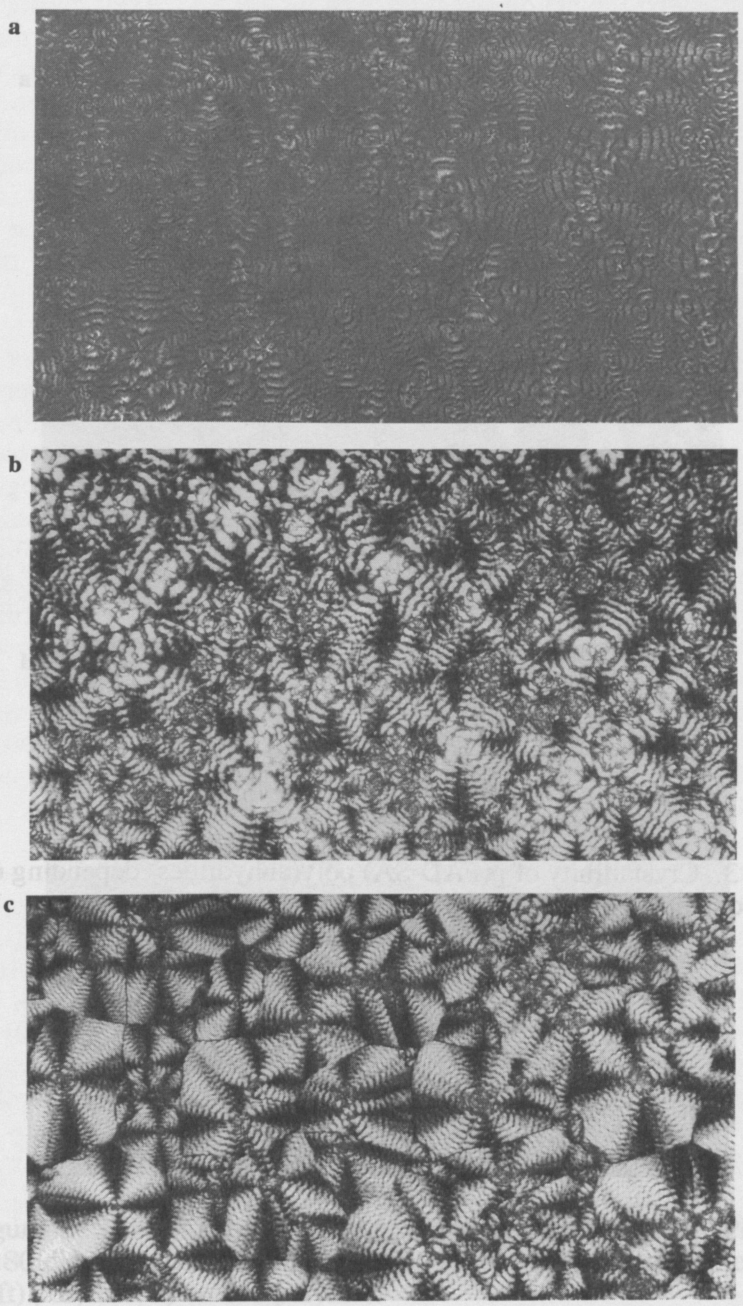

Figure 2. Polarized light microscopic pictures of poly(anhydride) films: a) pSA (250x), b) p-(FAD-SA) 20:80 (400x), c) p-(FAD-SA) 50:50 (400x).

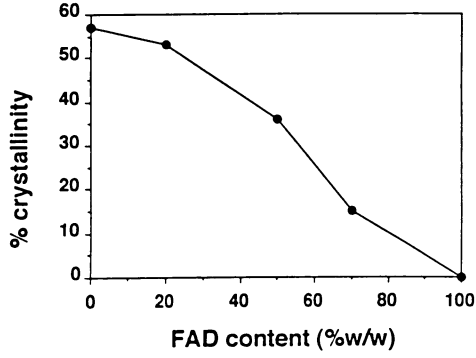

Figure 3. Crystallinity of p(FAD-SA) poly(anhydrides) depending on FAD content.

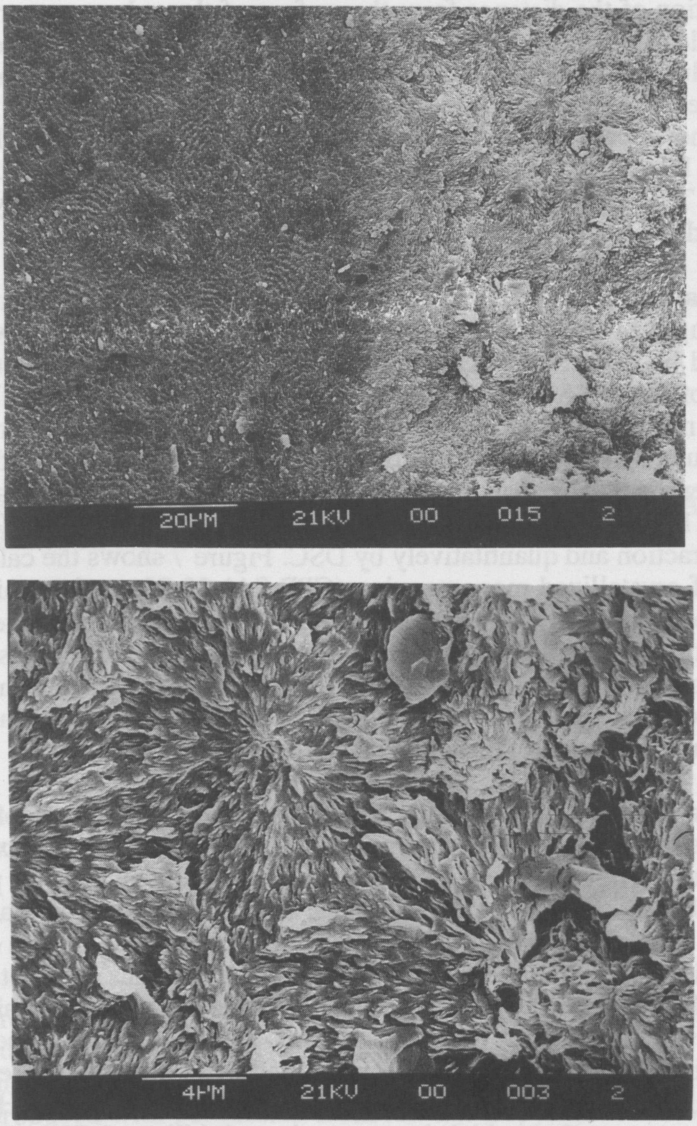

Figure 4. SEM pictures of cross sections through eroded p(CPP-SA) 20:80 dics: a) erosion front separating eroded(right) from non-eroded (left) polymer, b) eroded polymer.

sis, we measured the pH on the surface of p(CPP-SA) 20:80 during erosion using confocal microscopy(*26*). Figure 6 shows the value for the pH as a function of the distance from the surface of the polymer matrix disc. The pH clearly drops when approaching the surface of the polymer. This effect is due to the high concentration of released monomers upon degradation. Keeping in mind the highly porous structure of the eroded zone of the polymer it can be hypothesized that the pH inside this network is determined by the monomers and is even lower than the pH at the surface(*26*). This issue is very important with respect to the stability of pH sensitive drugs such as some proteins or peptides.

Changes in Crystallinity. From the structural changes during erosion, changes in polymer crystallinity could be suspected. They were investigated by differential scanning calorimetry and x-ray diffraction. In the case of the p-SA homopolymer, it was found that the crystalline regions are more resistant towards degradation than the amorphous regions. These results agree with the SEM pictures obtained from the degraded part of polymer discs. The monomers SA and CPP were found to crystallize to relatively high extents in all polymers qualitatively shown by wide-angle x-ray diffraction and quantitatively by DSC. Figure 7 shows the calculated amount of crystallized monomers in p(CPP-SA) 20:80, as determined by DSC according to (*26*). The presence of crystallized material proves indirectly that the pores of eroded polymer are filled with a saturated solution of monomers. FAD monomer is liquid at room temperature and therefore not able to crystallize upon release. Due to its low solubility in aqueous buffer solution, however, it sticks to the eroding discs as a film.

The Release of Monomers during Erosion. The release of acidic monomers indicates the importance of pH during erosion. As an example, the release profile of SA and CPP monomer during the erosion of p(CPP-SA) 20:80 is shown in Figure 8. The release profile of SA is similar to the release of substances from monolithic devices. The release profile of CPP is discontinuous as the release rate increases after SA has completely left the eroded polymer matrix. This spontaneous increase can be explained by the higher solubility of SA compared to CPP. The dissolved SA, therefore, controls the pH inside the pores of the eroded zone limiting, thereby, the solubility of CPP. After SA has been completely released, the pH inside the pores starts to rise, which increases the solubility of CPP(*26*). This process finally increases the release rate of CPP from the eroded polymer matrix.

Modeling Polymer Erosion. The modeling of polymer erosion is the first step towards the theoretical design of controlled release systems with an a priori adjusted release rate. The lack of knowledge about erosion, however, hindered the development of models substantially. The first attempts

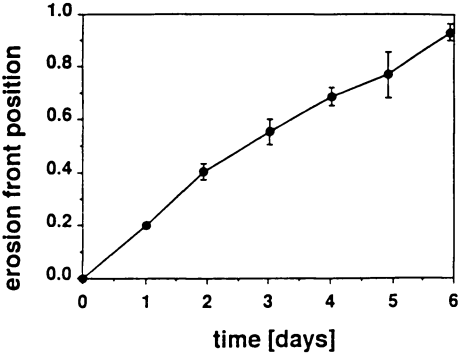

Figure 5. Relative position of the erosion front in p(CPP-SA) 20:80 depending on time.

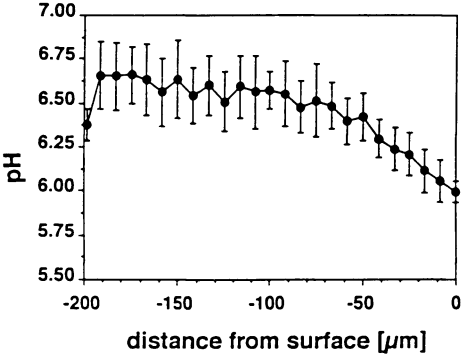

Figure 6. pH in the degradation medium as a function of distance to the surface of a p(CPP-SA) 20:80 polymer disc after 2 days of erosion in daily changed 0.1 M phosphate buffer pH 7.4 at 37°C. (Reproduced with permission from ref. 26. Copyright 1993 Wiley & Sons.)

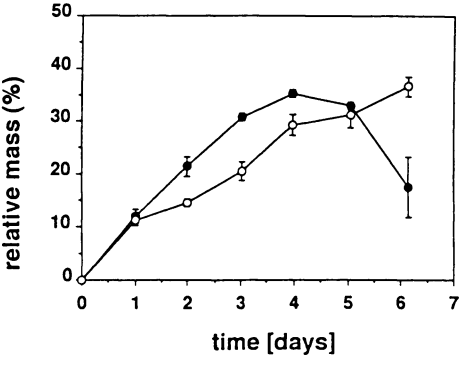

Figure 7. Content of crystallized monomers in a p(CPP-SA) 20:80 matrix during erosion: o CPP, • SA.
(Reproduced with permission from ref. 26. Copyright 1993 Wiley & Sons.)

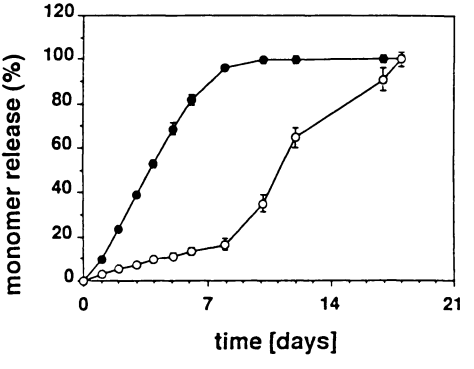

Figure 8. Release of monomers during the erosion of a p(CPP-SA) 20:80 polymer matrix disc: o CPP, • SA.
(Reproduced with permission from ref. 26. Copyright 1993 Wiley & Sons.):

to describe the erosion of biodegradable polymers stem from the description of the dissolution of erodible tablets(*27*). It was assumed that erosion could be described by surface dissolution kinetics. Later, diffusion processes were taken into account and modeled as a pseudo-steady state process, where erosion was modeled assuming first order kinetics or a constantly moving erosion front(*28-29*). Introducing non-steady state analysis, erosion was described as a moving front problem with constant velocity(*30*). All these models describe erosion in one dimension and do not allow descriptions of the microstructural changes upon erosion. Inspired by the two-dimensional description of the dissolution of matrix tablets(*31-32*), a two-dimensional model able to describe the structural changes of our investigated polymers upon erosion was developed. Rather than taking individual factors of polymer erosion into account, we combined them by regarding the erosion of small parts of polymer matrix as a random event(*33*).

The Basic Concept. A polymer matrix was represented by a two-dimensional computational grid, in which each grid point represents either an amorphous or crystalline part of the polymer matrix. The erosion of such a 'polymer pixel' was assumed to depend on two features: the contact of the polymer with the degradation medium, and the crystalline or amorphous nature of a matrix part which is represented by a pixel. Polymers not in contact with water will not erode. Pixels on the surface of the polymer matrix or next to an eroded neighbor have contact to water. The erosion of crystalline matrix parts occurs at a slower rate than amorphous parts, a characteristic which was observed in the structural studies(*26*). Besides these fundamental assumptions, a general algorithm must be defined to develop a working model: the matrix must be represented by a computational grid divided into individual pixels. A distribution must be chosen for crystallites and amorphous parts. After contact with an eroded neighbor, each pixel is assigned an individual life expectancy after which it is regarded eroded. The life expectancies are distributed according to a first order Erlang distribution(*34*) from which they are chosen randomly. To account for the crystalline or amorphous nature, different constants are chosen for use in the Erlang distribution.

The Representation of a Polymer Matrix. To represent a polymer matrix prior to erosion, it is sufficient to represent only a cutout of the matrix, if the erosion problem is symmetrical. Figure 9 shows such a cutout for a cross section through a cylindrical matrix.
To account for the crystallinity, some of the pixels have to be designated to represent crystalline polymer matrix parts. In the easiest case, a random distribution of them can be assumed:

$$c(x_{ij}) = \begin{cases} 1-\chi & x_{ij}=0 \\ \chi & x_{ij}=1 \\ 0 & \text{all other values} \end{cases} \quad \begin{array}{l} \text{for:} \\ 1 \le i \le n_x, \\ 1 \le j \le n_y. \end{array} \qquad (1)$$

χ is the crystallinity of the polymer. The status x_{ij} (1 for crystalline and 0 for amorphous) of all pixels is assessed from consecutive Bernoulli trials(*35*). $c(x_{ij})$ is the probability that a pixel at location x=i and y=j on the grid represents an amorphous or crystalline part of the matrix. Figure 10a shows the theoretical representation of a polymer matrix prior to erosion. Dark pixels represent crystalline, whereas white pixels represent amorphous parts of the polymer.

The Simulation of Erosion. After having set up the grid, the erosion algorithm can be applied. A first order Erlang distribution(*34*) was used for the calculation of the life expectancy of a pixel after its contact with water

$$e(t) = \lambda * e^{-t*\lambda} \qquad (2)$$

e(t) is the probability that a pixel degrades after a time t. Random variable t is the time that elapsed between the first contact with water and the erosion of the pixels. λ can be considered as a rate constant and is different for amorphous and crystalline pixels. To achieve results independent from the grid size, the grid size n has to be taken into account in equation 2:

$$e_n(t) = \lambda * n * e^{-t*\lambda*n} \qquad (3)$$

Using Monte Carlo sampling techniques(*36*), the life expectancy of an individual pixel can now be calculated from equation 3. Erosion begins at the pixels that represent the surface of the polymer matrix. Their lifetime is calculated and the pixel with the shortest lifetime is determined. Erosion proceeds with the removal of eroded pixels from the grid, now considered to represent aqueous pores. They then initiate the erosion process of non-eroded neighbors, the life expectancies of which are calculated(*33*). The next pixel is eroded, and so on. As an example, the erosion of the grid shown in Figure 10a can be seen in Figure 10b. In contrast to Figure 10a dark pixels represent non-eroded polymer and white pixels eroded polymer. The appearance of the cross sections of eroded discs shown in Figure 4a agrees with the appearance of the lattice during erosion. In both cases, the erosion front is clearly visible.

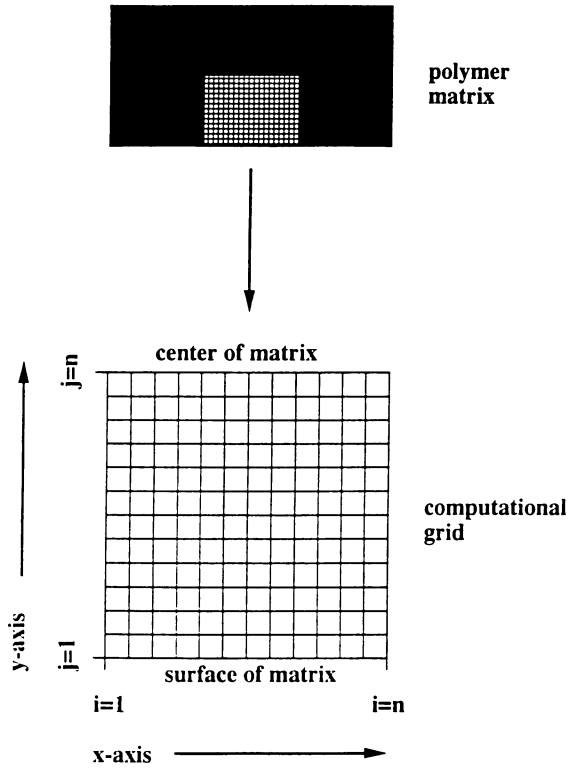

Figure 9. Representation of a polymer disc by a computational grid. (Reproduced with permission from ref. 33. Copyright 1993 ACS.)

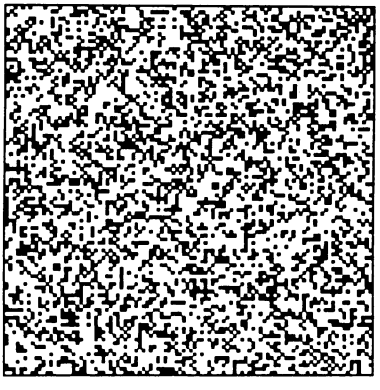

Figure 10a. Theoretical representation of a polymer matrix: prior to erosion (dark pixels = crystalline areas, white pixels = amorphous areas). (Reproduced with permission from ref. 33. Copyright 1993 ACS.)

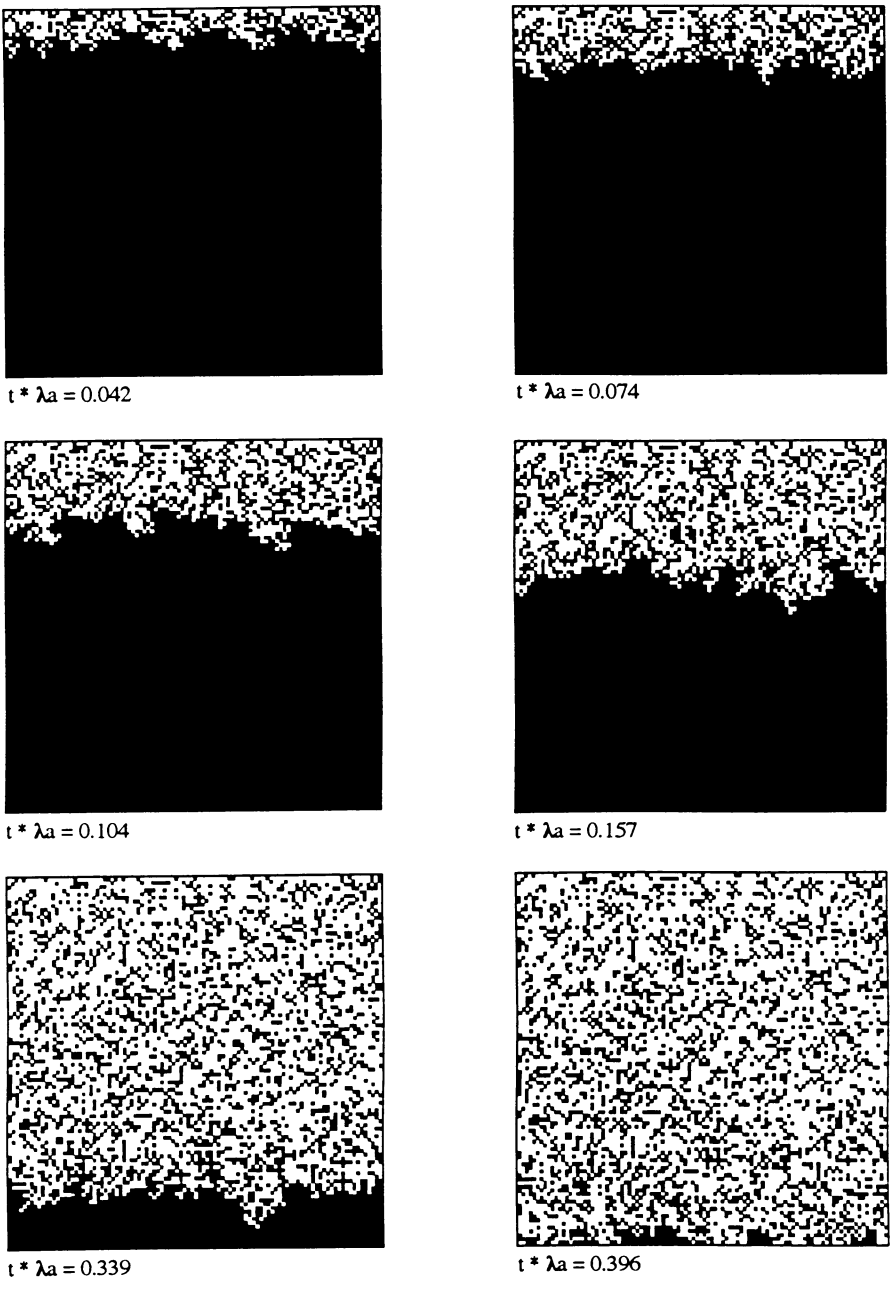

Figure 10b. Theoretical representation of a polymer matrix: changes during erosion (dark pixels = non-degraded areas, white pixels = degraded areas). (Reproduced with permission from ref. 33. Copyright 1993 ACS.)

The Quantitative Evaluation of Experimental Results. The unknown parameters in this model are the erosion rate constants for amorphous and crystalline pixels. Once these parameters are known the model becomes a tool to estimate the erosion behavior of polymer matrices and to predict when the last portion of drug will be released. The computational grid can, thereby, be fit to any desired shape.

In order to determine the erosion rate constants, system parameters must be defined to develop a model to fit the experimental data. Therefore two functions were chosen:

$$f(t) = \frac{1}{n} \sum_{i=0}^{n} f_i(t) \tag{4}$$

$$m(t) = \frac{1}{n^2} \sum_{i=1}^{n} \sum_{j=1}^{n} s(x_{ij}) \tag{5}$$

Equation 4 defines the position of the erosion front f(t) at time t as an average value of the position $f_i(t)$ of the foremost eroded pixel in each column of the grid. Experimentally, the position of the erosion front was determined by SEM. Equation 5 calculates the remaining mass of the matrix m(t) at time t, $s(x_{ij})$ being equal to 1 for non-eroded pixels and 0 for eroded pixels. Experimentally, the remaining mass was determined by weighing dried eroded polymer matrix discs. Using equations 4 and 5, the model was fit to experimental data of p(CPP-SA) 20:80 and p(CPP-SA) 50:50, minimizing the squared distances between experimental points and simulated data calculated from equation 4 and 5 (*37-38*). As shown in Figures 11 a and b, the movement of the erosion front is almost linear in both polymers. The larger deviation between experimental and predicted data for p(CPP-SA) 50:50 (cf. Fig. 11b) is mainly due to problems in the determination of erosion fronts in this polymer by light microscopy. The loss of mass after an induction period also follows linear kinetics. From the good fit to this parameter it can be assumed that the effect of the error in the determination of the erosion front movement has only moderate effect on the determination of the rate constants. The erosion rate constants obtained are shown in Table I.

As expected from the structural information on eroded polymer matrices, the erosion rate constants for crystalline pixels are substantially lower

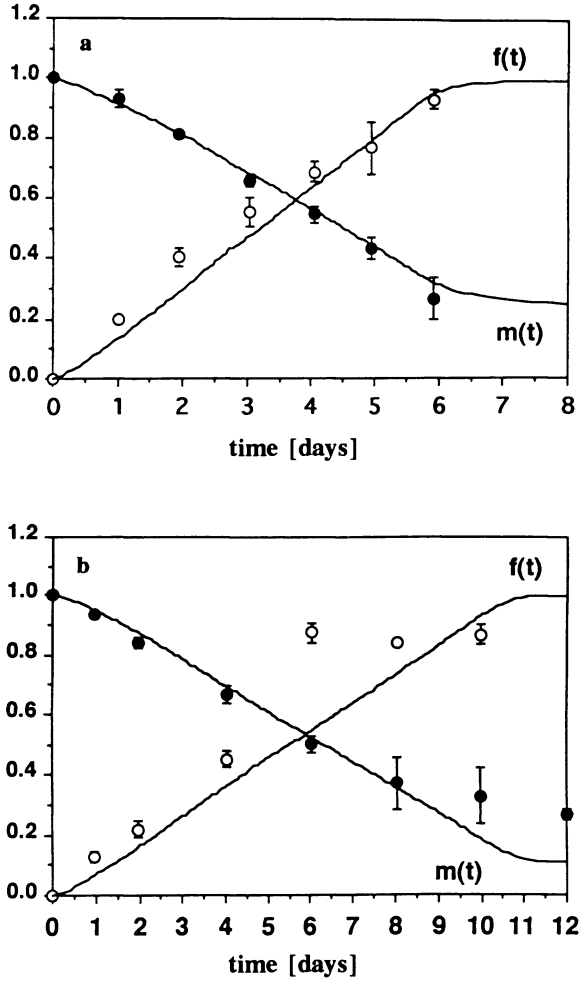

Figure 11. Fit of theoretical functions for mass loss and erosion front movement to experimental data: a) p(CPP-SA) 20:80, b) p(CPP-SA) 20:80.
(Reproduced with permission from ref. 33. Copyright 1993 ACS.)

Table I. Erosion rate constants for crystalline and amorphous areas in two poly(anhydrides)

	λ_a [s^{-1}]	λ_c [s^{-1}]
p(CPP-SA) 20:80	$7.32*10^{-7}$	$8.75*10^{-9}$
p(CPP-SA) 50:50	$2.7*10^{-7}$	$3.85*10^{-11}$

Source: Reprinted with permission from ref. 33. Copyright 1993.

compared to the rate constants for amorphous pixels. The obtained microconstants allow the simulation of erosion of any kind of polymer matrix cross section under various boundary conditions. A good example is the simulation of erosion of devices partially coated with a water impermeable coating. Such devices could be very useful for the modification of release profiles for slowing down the overall erosion velocity of a biodegradable device.

The Consequences for the Release of Proteins from Polymers. The erosion of the poly(anhydrides) follows a well defined pattern. All polymers degrade from the surface of the polymer matrix discs towards their center. A moving front sharply separates eroded from non-eroded polymer. It could be shown by scanning electron microscopy that crystalline areas of the polymers are more resistant to erosion than amorphous areas. Due to the spherulitic microstructure of the polymers (cf. Figure 2), erosion creates highly porous devices consisting of the crystalline skeleton of eroded spherulites. Due to the high degradation rates, many oligomers and finally monomers are released. Reaching the limit of solubility, these substances start to precipitate out of solution, which was observed by wide angle x-ray diffraction and differential scanning calorimetry. Substantially high amounts of monomers were found to be in a crystalline state(*26*). Confocal fluorescence microscopy showed that the pH on the surface of the polymers during erosion was lower than in the buffer medium. From the presence of crystalline monomers inside the erosion zone, it can be concluded that the aqueous phase inside the polymers is saturated with monomers. As SA has the highest solubility of all monomers, this compound determines the pH. From the pKa which is about 4.5 and the solubility which is 0.011M, the theoretical pH minimum is about 3.5(*39*). Due to the diffusion of hydroxide ions from the degradation medium into the erosion zone, however, some of the free acids are neutralized, which buffers the pH probably around the pKa. Buffer salts like HPO_4^{2-} are apparently not able to raise the pH inside the porous zones of the eroded

discs. The major reason is the long diffusion pathway into the disc along which they get steadily protonated by dissolved monomers and lose their potential to raise pH. The monomer saturated solution inside polymer pores with a pH of approximately 4.5 is, therefore, the environment that proteins and peptides will be in contact prior to release out of the matrix. Once the stability data of such a biomolecule is known, it can readily be decided whether these types of polymers will make suitable drug carriers. The well defined erosion behavior of the investigated polymers allows the development of mathematical models that describe changes in polymer microstructure during erosion(*33*). Once fit to experimental data, these models are a useful tool to predict changes in polymer microstructure. They describe important parameters like porosity, loss of weight, eroded polymer area and may, therefore, become an important tool to predict the release kinetics of proteins and peptides from such polymers in the future.

Controlled Release Devices for the Delivery of Proteins and Peptides from Polymers

For the delivery of proteins and peptides, non-degradable and biodegradable polymers have been used in controlled release. Due to the high molecular weight of proteins, direct diffusion through a non-degradable polymer matrix is not possible(*40*). By the introduction of a network of pores in manufacturing, however, the release of such large compounds does occur(*41*). Another possibility is the creation of hydrophilic pathways using swellable polymers, or embedding the compounds into gels. In the case of biodegradable polymers, pores are created upon erosion of the polymer matrix enabling the release of proteins from the dosage form. All of these options have certain advantages and disadvantages. Embedding suspended compounds into a non-degradable matrix prevents some of the protein from being released(*42*), or might cause some instabilities due to the intense contact with organic solvents(*43*). Their disadvantage with respect to parenteral application, however, is the need for removing such systems after therapy. By using gels as a carrier, the protein may be released very quickly if not combined with some other sort of material(*44-45*). Degradable polymers change their properties substantially during erosion, a characteristic which may or may not be beneficial for the stability of proteins and peptides. In general, decisions about the suitability of a release device for specific proteins or peptides and appropriate manufacturing technology must be made on a case by case basis. In the following section, we provide a number of examples from the progress we made in the delivery of proteins from polymers.

Biodegradable Polymers for Immunization. The idea of using polymers as antigen releasing carriers for the stimulation of immune responses

emerged in the seventies (*46*). Due to their ease of application and the progress in their development, microspheres emerged as a potentially efficient carriers to enhance the immune response (*47*). They have so far been used for a number of vaccines (*48-50*). These microspheres were made from polymers based on poly-lactic acid (PLA) and its copolymers with glycolic acid (PLGA). For these applications, loading a polymer with a high molecular weight protein requires adjusting the desired release rate and preventing the protein's loss of activity.

In an attempt to develop a controlled release system for vaccination against tetanus, we investigated the design of microspheres with a desired release rate and methods to maintain the imunogenicity of the processed tetanus toxoid(*51*). For the manufacturing of microspheres, the solvent evaporation and solvent extraction methods were applied to the double emulsion technique. The solvent evaporation method has been used successfully for the encapsulation of hydrophilic drugs and peptides(*52-53*) and was recently applied to the encapsulation of proteins(*54*). According to the protocol, 50μL of saline tetanus toxoid solution (3600 Lf/mL) was emulsified by vortex mixing in 1mL organic solution (methylene chloride or ethyl acetate) containing 200 mg of polymer. The emulsion was homogenized by sonication and dispersed into 1mL of a 1% aqueous PVA solution by vortex mixing. The final double emulsion was diluted by adding it to 100 mL of a 0.3% PVA solution while stirring with a magnetic stirrer. The organic solvent was then allowed to evaporate for 3 hours (solvent evaporation) or extracted by adding 200 mL of 2%(V/V) aqueous isopropanol solution (solvent extraction). Both techniques produced microspheres with a high loading capacity (>80%). Critical points in the encapsulation procedure are the protein stability upon contact with moisture(*55*) and organic solvent (*43*) during the formation of the emulsion as well as the subsequent freeze drying.

Protein stability under the manufacturing conditions was investigated varying three parameters. We varied the type of solvent for the dissolution of polymer using methylene chloride and ethyl acetate and investigated the effect of three different types of stabilizers: Pluronic F68, PEG 4,600 and sodium glutamate. To mimic the conditions that prevail during the manufacturing of microspheres, emulsions were prepared from 100μL aqueous tetanus toxoid solution and dispersed it in 1mL of organic solvent. These emulsions were freeze dried and investigated for aggregation by HPLC(*56*). Table II shows the results from this study.

Table II gives a good survey on the impact of manufacturing conditions on the stability of the protein. Sample one shows that moisture alone causes

Table II. manufacturing conditions and their effect on protein aggregation

Set of conditions	Solvent	Stabilizer	Aggregation (%)
1	none	none	14
2	none	Pluronic F68	0
3	none	PEG 4,600	3.9
4	none	Sodium Glutamate	4.4
5	Methylene chloride	none	13.11
6	Methylene chloride	Pluronic F68	9.6
7	Methylene chloride	PEG 4,600	9
8	Methylene chloride	Sodium Glutamate	3.4
9	Ethyl acetate	none	5.4

the protein to aggregate substantially. The impact of even small amounts of moisture on the structure of lyophilized proteins can be tremendous(*55*). The aggregation of the protein in methylene chloride (sample 5) is higher than in ethyl acetate (sample 9) which is unfortunately the poorer of both solvents for many biodegradable polymers. The use of stabilizers like Pluronic F68 might be benefical in preventing some of the proteins and peptides from aggregating or from adsorbing to hydrophobic surfaces i.e. polymer forming the microspheres. This has been reported for a number of surfactants(*57*).

The goal for the release of tetanus toxoid from microspheres was continuous release over a period of weeks. For that purpose two types of polymers were used: L-PLA and D,L-PLGA1:1. The PLGA polymers are amorphous whereas L-PLA are crystalline. Depending on their molecular weight they erode in weeks or months(*58*). To investigate the effect of erosion velocity the polymers were chosen with a molecular weight of either 100,000 or 3,000 Da. The release was studied by incubation of the microspheres in phosphate buffer pH 7.4 at 37°C. Due to the slow degradation of the polymers it was sufficient to replace the buffer at least every 5 days. The released protein was determined by using a microBCA protein assay. The results for the two types of polymers are shown in Figure 12a and b. The release rate was clearly affected by polymer composition with PLGA faster than from PLA at the same molecular weight. In both cases,

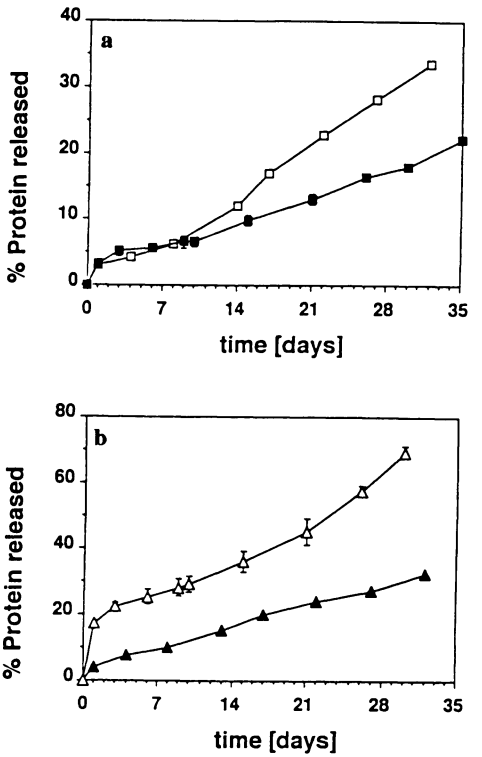

Figure 12. In vitro release of tetanus toxoid from different types of polymer:
a) ■ PLA (Mw 100,000); □ PLGA (Mw 100,000)
b) ▲ PLA (Mw 3,000); △ PLGA (Mw 3,000)
(Reproduced with permission from ref. 56. Copyright 1993 Butterworth-Heinemann Ltd.)

the release from the low molecular weight polymers is faster. This result is due to the smaller size of microspheres prepared from these polymers since the organic polymer solution had a lower viscosity. Other reasons could be their faster degradation due to differences in molecular weight. All preparations release over a period of weeks, as was intended. With the exception of low molecular PLGA, there is no substantial burst effect as reported for other vaccine preparations (*59*).

A general disadvantage of methods that use chemical reactions or physical interactions like chromatographic methods for the determination of protein concentrations is the lack of structural information. We, therefore, tested the *in vivo* response to the encapsulated tetanus toxoid by injecting the microspheres subcutaneously into mice. The sera was assayed for the antitoxin units using the toxin neutralization test(*60-61*) as well as an ELISA test. Figure 13a and b show the results for all microspheres as well as a control injection of fluid toxoid and aluminum adsorbed toxoid. The use of microspheres increases the immune response compared to the fluid toxoid. The use of aluminum adsorbed toxoid produces initially higher antitoxin titers which decrease, however, more rapidly compared to the encapsulated toxoid. The levels resulting from microsphere injection are considerably higher than the estimated minimum protective level which is about 0.01 AU/mL(*62*). The antibodies determined by the neutralization test and the IgG antibodies reach their maximum at different times. This could be explained by the induction of progressive affinity maturation tetanus antibodies induced by prolonged exposure to low concentrations of tetanus toxoid.

Protein Delivery from Poly(anhydride) Microspheres. A major problem associated with many dosage forms for drug release is the release of large amounts of the drug during initial stages of release known as the initial burst-effect. For microspheres, this burst effect tends to be enhanced since microspheres have a larger surface area to volume ratio than more sizable slabs. In addition, the change of biological activity of proteins can occur during microsphere formulation because of their sensitivity to environmental alternation. Our goal in this study was to prepare poly(anhydride) microspheres which permitted the controlled release of biologically active proteins without any initial burst in release. We selected two enzymes, trypsin (Mw24,000) and heparinase (Mw43,000) in addition to BSA (Mw 62,000) which has been used as a model protein. The measurement of enzymatic activity allowed us to investigate the effect of microsphere formulation on protein activity.

We encapsulated proteins into poly(anhydride) microspheres with the solvent evaporation method by using a double emulsion (*54*). However, this technique comprises of a number of formulation processes which may affect protein activity: contact of aqueous protein solution with

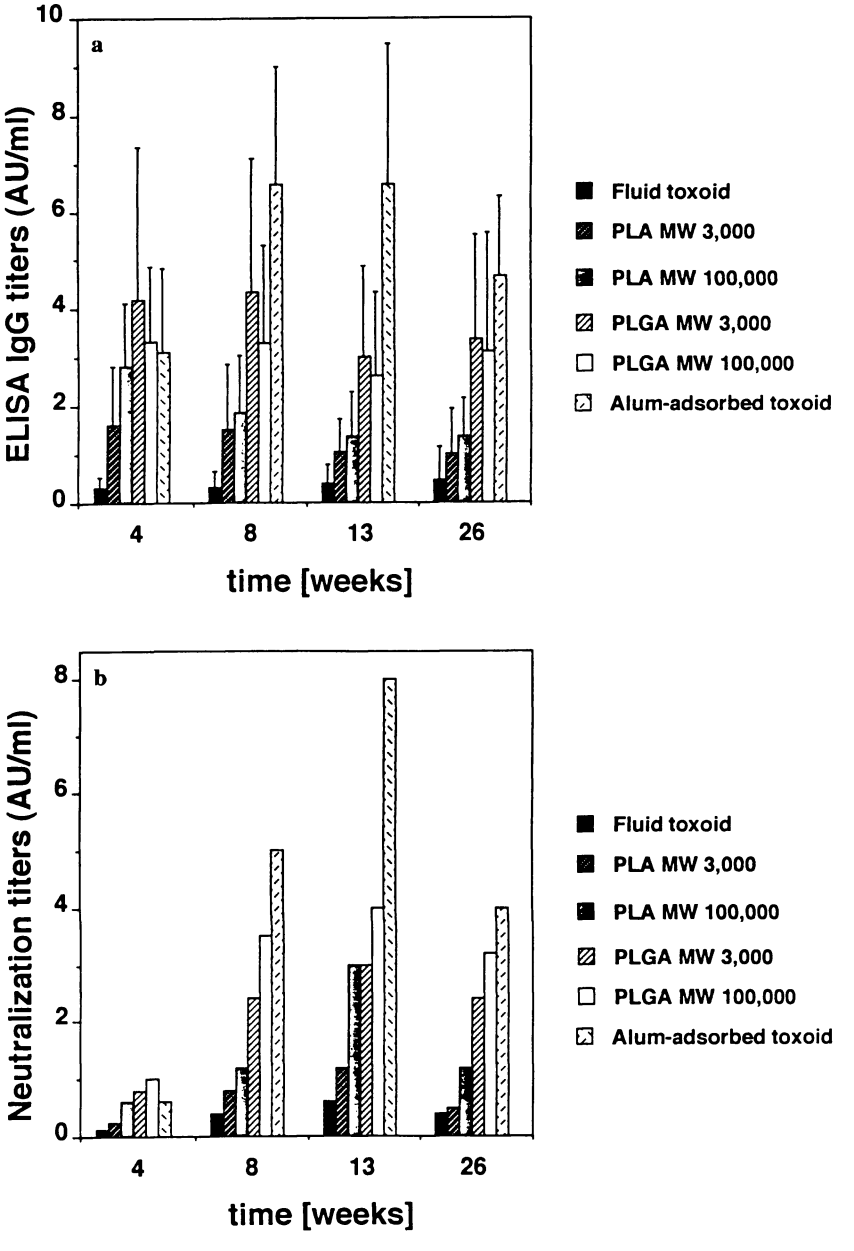

Figure 13. Results from the *in vivo* test of tetanus toxoid loaded microspheres:
a) *In vivo* neutralizing antibody response (antitoxin units/ml serum),
b) IgG antibody response by ELISA.
(Reproduced with permission from ref. 56. Copyright 1993 Butterworth-Heinemann Ltd.)

the organic phase, vortex mixing, exposure to ultrasound and freeze drying.

The activity loss of proteins was measured based on the specific activity of proteins at each stage of the process (*63*). Table III shows the effect of the formulation process on the enzymatic activity of trypsin.

Table III. Activity loss of trypsin after each step of microsphere preparation

Preparation step	remaining activity (%)
Trypsin solution	100
vortex mixing	100
sonication for 30s	59
3 h solvent evaporation	56
freeze drying	59

The sonication process which was performed in presence of the organic solvent to prepare a primary emulsion, causes the main activity loss of protein, while freeze-drying did not have any addition effect. It is known that ultrasound has an effect on the biological properties of proteins in aqueous solution due to a number of factors such as temperature, mixing and cavitation(*64*). Table IV shows the effect of ultrasound exposure period on the activity loss of proteins during microsphere preparation together with the additional effect of some protein stabilizers(*65*).

Table IV. Activity loss of trypsin during microsphere preparation (*66*)

Period of sonication [s]	Type of stabilizer	Amount of stabilizer (% w/w)	remaining activity
10	none	-	80.5
20	none	-	67.3
30	none	-	58.9
30	BSA	5	58.6
30	BSA	10	58.1
30	Glycine	4	58.7*
30	Glycine	7.5	59.8*
30	Glycine	8	56.6*
30	Glycine	15	57.2*

*Differences within the error margin of the test

The extent of activity loss becomes smaller with a decrease in the exposure period of sonication. In addition, the decreased period did not reduce the size of the primary emulsion. These findings demonstrated that the observed activity loss results from the sonication probe and not from the increase in the interfacial area between aqueous and organic phase. Little effect of the stabilizers used here on activity loss was observed, indicating the poor potential of these substances to protect the investigated proteins against ultrasound exposure. Trypsin and heparinase were encapsulated to study the enzymatic activity of proteins in poly(anhydride) microspheres. Figure 14 shows the comparison of the remaining activity between the proteins encapsulated in microspheres and the proteins in a soluble form after incubation in phosphate buffer pH 7.4 at 37°C. At different stages of the experiment, the remaining % activity of proteins in microspheres was assessed by determining the activity of protein that could be extracted from these systems (*66*) These results clearly indicate that encapsulation of proteins inside poly(anhydrides) may stabilize their activity for a short period of time (1-2days).

Figure 15 shows release profiles of BSA from p(FAD-SA) 25:75 at various protein loadings. No initial burst is observed irrespective of the protein loading. The protein is released for up to three weeks at a near-constant rate.

The release rate of protein depends on the monomer composition of poly(anhydrides) used as can be seen from Figure 16. Release periods of several days to a couple of weeks are possible for poly(anhydride) microspheres by changing their monomer composition(*66*).

Biodegradable Injectable Nanospheres Composed of Diblock Poly(ethyleneglycol)-Poly(lactic-co-glycolic acid) Copolymers A major challenge in the area of parenteral administration of drugs is the development of a drug carrier that is small enough for intravenous application and which has a long circulation half-life. There are numerous potential applications for such a system: the suppression of toxic side effects which can occur when the drug is injected in the form of a solution, or the protection of sensitive compounds against degradation in the plasma. Consequently there have been many approaches to develop such systems (*67-68*). The major obstacle in the use of injectable systems is the rapid clearance from the blood stream by the macrophages of the reticulo-endothelial system (RES). Polystyrene particles as small as 60 nm in diameter, for example, are cleared from the blood within 2 to 3 min(*69*). By coating these particles with block copolymers based on polyethylene glycol and polypropylene glycol, their half-life was significantly increased (*70*). Polystyrene particles are, however, not biodegradable and are not therapeutically useful. For this reason, only liposome systems have been developed for intravenous administration *(71-76)*. Due to their small size they were expected

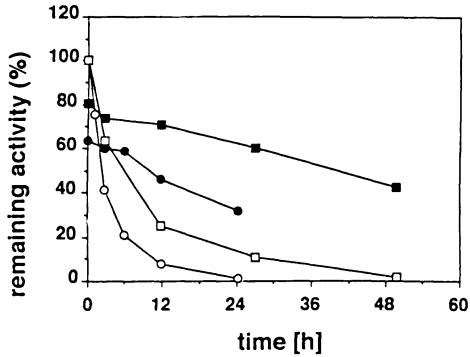

Figure 14. Stability of Heparinase and Trypsin with and without polymer encapsulation in phosphate buffer pH 7.4: ○ Heparinase solution, ● Heparinase encapsulated, □ Trypsin solution, ■ Trypsin encapsulated.
(Reproduced with permission from ref. 66. Copyright 1993 Plenum Press.)

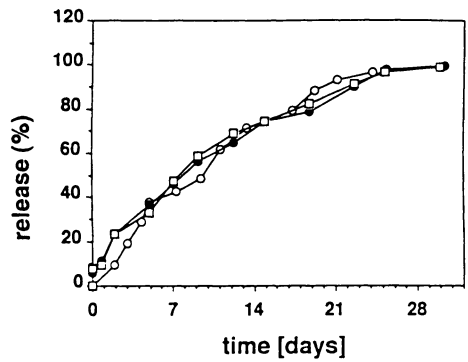

Figure 15. Release of BSA from poly(anhydride) microspheres depending on loading: ○ 1% BSA, ● 2% BSA, □ 4% BSA.
(Reproduced with permission from ref. 66. Copyright 1993 Plenum Press.)

to freely circulate in the blood. It has been found, however, that they are cleared from the blood by uptake through the reticulo-endothelial system (RES). The coating of liposomes with poly(ethyleneglycol) (PEG) increased their half life substantially (*71-77*). The presence of the flexible and relatively hydrophilic PEG chains induces a steric effect at the liposome's surface, thus reducing protein adsorption and RES uptake (*77*).

Rather than using liposomes, we designed PEG-coated biodegradable nanospheres that consist of polymer only(*78*). These are among the first degradable polymer-based systems with potential use for prolonged intravenous administration or drug targeting.

The 'ideal' nanosphere (Figure 17) is biodegradable, biocompatible, has a size of less than 200 nm, and has a rigid biodegradable core. The PEG-coated surface theoretically provides a prolonged half-life in the blood by masking it from the RES. We chose the FDA approved polyesters poly(lactic-co-glycolic acid) (PLGA) to form the core of the particles. These polymers allow us to adjust erosion rates and therefore drug release by changing the monomer ratio. We synthesized a series of diblock copolymers PLGA-PEG, starting with PEG of various chain lengths and progressively increased the chain length of PLGA. Stannous octoate was used as a catalyst for the ring-opening polymerization of lactide and glycolide in the presence of monomethoxy polyethylene glycol (MPEG; Mw 5,000; 12,000 and 20,000). The polymers obtained were characterized by nuclear magnetic resonance spectroscopy (NMR), gel permeation chromatography (GPC), infrared spectroscopy (IR), differential scanning calorimetry (DSC) and X-ray diffraction. The polymerization reaction was followed by GPC from which molecular weight and polydispersity were determined. The consumption of lactide and glycolide can be observed from a decrease of peak D (Figure 18). The shifting of the peak P towards lower retention times (higher molecular weights) indicates that an addition reaction takes place at the hydroxyl end group of the PEG chains. The polydispersity remains low during the polymerization (Mn/Mw less than 1.1). Both the crystallinity and the glass transition temperature (Tg) were determined by using DSC. The diblock copolymers show a single Tg, which shifts to higher temperatures with an increase of the PLGA chain length inside the PLGA-PEG (Figure 19). A complete discussion of the DSC results can be found elsewhere(*79*). Random lactic acid-ethylene oxide copolymers show two distinct Tg's (*80*), suggesting a phase separation inside the polymer. We suppose that the single Tg we observed is due to an entanglement effect of long PEG and PLGA chains in the polymers, which cannot easily phase-separate. The exact chemical composition of the polymers was determined by ^{13}C NMR spectroscopy.

Sterically stabilized particles were prepared from diblock PLGA-PEG copolymers or from blends of PLGA and PLGA-PEG. These polymers were dissolved in a common solvent (ethyl acetate or methylene

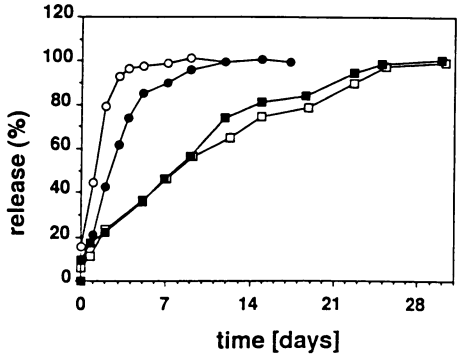

Figure 16. Release of BSA from poly(anhydride) microspheres depending on polymer type: o p(SA), ● p(FAD-SA) 8:92, □ p(FAD-SA) 25:75, ■ p(FAD-SA) 44:56.
(Reproduced with permission from ref. 66. Copyright 1993 Plenum Press.)

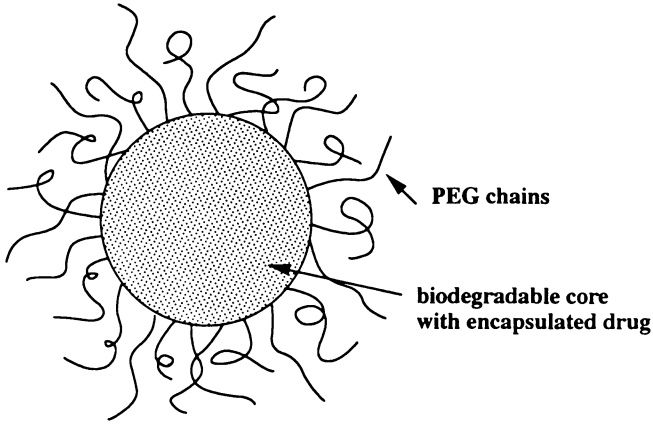

Figure 17. Schematic representation of an 'ideal' nanosphere having a biodegradable drug containing core and a coating of Polyethylene glycol chains.

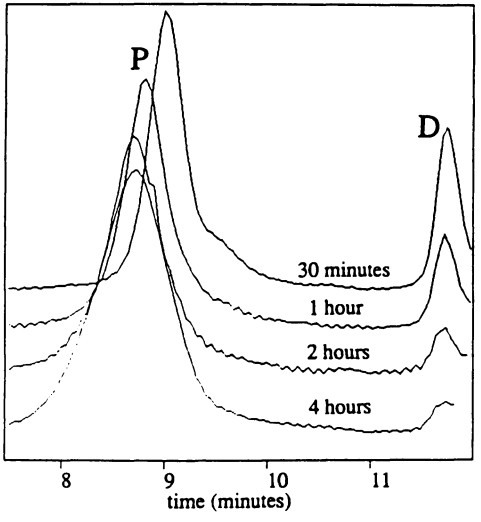

Figure 18. ATime course of the polymerization reaction between PEG and lactide/glycolide followed by GPC: Peak P: polymer PEG-PLGA, peak D: starting material (glycolide+lactide).

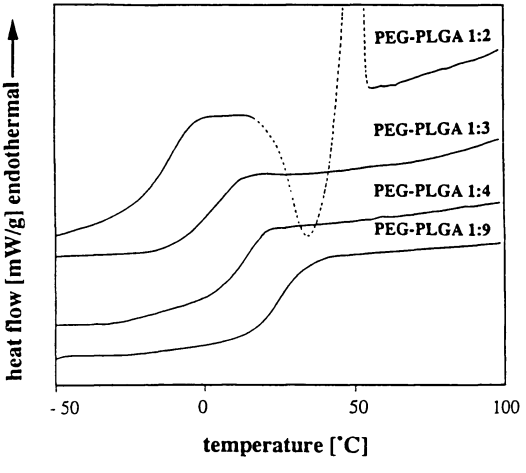

Figure 19. DSC thermograms of PLGA-PEG diblock copolymers (heating rate 10 °C/min, MW PEG=5000, for increasing chain length of PLGA).

chloride). An O/W emulsion was formed by vortex mixing and sonicating for one minute. The organic solvent was then slowly evaporated, at room temperature, under gentle stirring for two hours. Slow removal of the solvent allows the reorganization of the polymer chains inside and on the surface of the droplets. By optimizing the viscosity of the organic phase, the volume ratio of the two phases and the sonication parameters, nanospheres of a mean size of about 150 nm were obtained. After removal of the organic solvent, the nanospheres were isolated from the aqueous phase by centrifugation. They could later be readily redispersed in water, probably due to the presence of PEG chains on their surface.

The nanospheres were characterized by various methods. The surface composition of lyophilized particles was determined by X-ray photoelectron spectroscopy (XPS). Figure 20 shows the carbon 1s envelopes that were observed by analyzing the nanosphere powder. One main carbon environment is observed for PEG. It corresponds to the ether carbon C-O (*81*). The spectrum of PLGA polymer (curve a) shows three main carbon environments. In the case of PEG-PLGA nanospheres, the peaks are still present. As the information obtained by XPS corresponds to the first layers on the nanosphere's surface (about 5 nm(*82*)), this spectrum indicates that PEG is present on the surface of the nanosphere powder. Moreover, we verified that PEG remains on the surface after incubation in distilled water for 24 hours at 37 °C.

To investigate the *in vivo* half life of the systems, the nanospheres were labeled with ^{111}Indium, which has been used for gamma-scintigraphy studies in humans (*83*). ^{111}In was attached directly to the polymer chain by complex formation following a method that has already been used for liposomes (*83*). The incubation at 37 °C in PBS or horse serum for more than 24 hours showed that there was less than 4 % label loss. This indicated that the label is bound tightly enough to prevent loss during *in vivo* study. Subsequently biodistribution studies were performed by injecting ^{111}In-labeled PLGA and PEG-coated nanospheres into the tail vein of Balb/c mice (18-20g). Five minutes after injection of uncoated PLGA nanospheres, 40% of nanosphere-associated ^{111}In radioactivity was found in the liver and approximately 15% in the blood. In the case of PEG-coated nanospheres, the results were reversed (15% of injected radioactivity in the liver, 60% in the blood). After four hours, 30% of the nanospheres were still circulating in the blood, whereas the PLGA nanospheres had disappeared completely from the blood.

These results are very encouraging and we hope that these nanospheres might be used as drug carriers for intravenous administration in the future. Studies are now underway to achieve the encapsulation of different hydrophobic drugs and small peptides into the core of these nanospheres. We are also determining the effect of PEG molecular weight

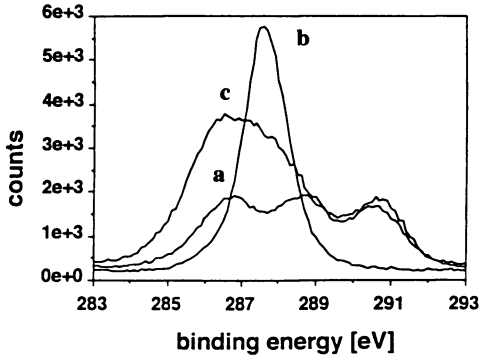

Figure 20. Surface analysis by XPS of PLGA powder: a) PLGA powder, b) PEG crystals, c) PLGA-PEG nanospheres.

and density on the RES uptake and on drug encapsulation efficiency and release.

Summary

Progress in various fields of protein delivery has been illustrated. Using poly(anhydrides) as a model we showed that it is possible to describe erosion mechanisms and to develop mathematical models of the complex processes involved in polymer degradation. Based on such models the design of delivery systems using computers might become possible in the future. Concerning manufacturing technologies for protein delivery, we showed how existing systems, like microspheres, can be improved and provided the development of vaccines as an example for future application of such systems. Finally the recent progress in the development of new dosage forms was illustrated with the example of biodegradable nanospheres with an increased circulation half-life. All these projects aim at a better understanding and an improved design of protein delivery systems.

Acknowledgments

The authors want to thank Dr. R.K. Gupta and Dr. G.R. Sieber for their contribution to the protein stability study and in the vivo immune response studies. Thanks are due to the Deutsche Forschungsgemeinschaft who sponsored the polymer degradation studies with grant No GO 565/1-1 and to the National Institutes of health who sponsored the same project with grant No. GM 26698. We thank Scios Nova for supplying us with polymers.

Literature Cited

1 Sadee, W., *Pharm. Res.* **1986**, 3, pp.3-6.
2 Luft, F.C.; Lang, G.R.; Aronoff, H.; Ruskoaho, M.; Toth, M.; Ganten, D.; Sterzel, R.B.; Unger, T. *J. Pharmacol. Exp. Ther.* **1986**, 236, pp.721-728.
3 Sluzky, V.; Tamada, J.A.; Klibanov, A.M.; Langer, R. *Proc. Natl. Acad. Sci.* **1991**, 88, pp.9377-9381.
4 Witkop B. *Adv. Protein Chem.* **1961**, 16, p.221.
5 Marcritchie *Adv. Protein Chem.* **1978**, 32, p.283.
6 Zhou, X.H.; Li Wan Po, A. *Int. J. Pharm.* **1991**, 75, pp.97-115.
7 Zhou, X.H.; Li Wan Po, *A. Int. J. Pharm.* **1991**, 75, pp.117-130.
8 Bawa, R.; Siegel, R.; Marasca, B.; Karel, M.; Langer, R. *J. Contr. Rel.* **1985**, 1, pp. 259-267.
9 Lee, P.I. In: *Treatise on controlled drug delivery*; Kydonieus, A. Ed.; Marcel Dekker Inc., NY, 1992; pp.155-195.
10 Heller, J.; Sparer, R.V.; Zentner, G.M. In: *Biodegradable Polymers as Drug Delivery Systems*, Chasin, M.; Langer, R. Eds., Drugs and the Pharmaceutical Sciences, Marcel Dekker, NY, 1990; Vol. 45, pp.121-163.
11 Tamada, J.; Langer, R. *J. Biomater. Sci. Polymer Edn.* **1992**, 3.4, pp. 315-353.
12 Samanen, J. M. In: *Peptide and Protein Drug Delivery*; Lee V., Ed.; Advances in parenteral sciences, Marcel Dekker Inc., NY, 1991; Vol. 4, pp137-167.
13 Siegel, R.; Langer R. *J. Contr. Rel.* **1990**, 14, 153-167.
14 Baker, R. W.; Controlled Release of Biologically Active Agents, John Wiley and Sons, NY, 1987; pp.84-131.
15 Joshi, A.; Himmelstein, K. J. *J. Contr. Rel.* **1991**, 15, pp.95-104.
16 Li, S. M.; Garreau, H.; Vert, M. *Journal of Materials Science: Materials in Medicine*, 1990, 1, pp.131-139.
17 Leong, K. W.; Brott, B. C.; Langer, R. *J. Biomed. Mater. Res.*, **1985**, 19, pp.941-955.
18 Li, S. M.; Garreau, H.; Vert, M. *Journal of Materials Science: Materials in Medicine*, **1990**, 1, pp.123-130.
19 Vert, M.; Li, S.; Garreau, H. *J. Contr. Rel.* **1991**, 16, pp.15-26.
20 Heller, J. *J. Contr. Rel.* **1985**, 2, pp.167-177.
21 Mathiowitz, E.; Ron E.; Mathiowitz, G.; Amato, C.; Langer, R. *Macromolecules* **1990**, 23, pp.3212-3218.
22 Tabata, Y.; Domb, A.; Langer, R. *J. Pharm. Sci.* **1993**, in press.
23 Langer, R.; Peppas, N., *J. Macromol. Sci.-Rev. Macromol. Chem. Phys.* **1983**, C23, pp.61-126.
24 Billmeyer, F. W. Textbook of Polymer Science, 3rd Edition, John Wiley & Sons, NY, 1984; pp. 273-281.

25 Tamada, J.A.; Langer R. *Proc. Natl. Acad. Sci. USA* **1993**, 90, pp.552-556.
26 Göpferich, A.; Langer, R. *J. Polymer Sci.* **1993**, 31, pp. 2445-2458.
27 Cooney, D. O. *AIChE Journal* **1972**,18.2, pp.446-449.
28 Baker, R. W.; Lonsdale, H. K. *Am. Chem. Soc. Div. Org. Coat. Plast. Chem. Prepr.* **1976**, 3, pp.229.
29 Heller J.; Baker R. W. In *Controlled Release of Bioactive Materials*; Baker, R. W., Ed., Academic Press, New York, 1980.
30 Thombre, A. G.; Himmelstein, K. J. *AIChE Journal* **1985**, 31.5, pp.759-766.
31 Zygourakis K. *Polym. Prepr. (Am. Chem. Soc., Div. Polym. Chem.* **1989**, 30.1, pp. 456-457.
32 Zygourakis K. *Chem. Eng. Sci.* **1990**, 45.8, pp.2359-2366.
33 Göpferich, A.; Langer, R. *Macromolecules* **1993**, 16, pp. 4105-4112.
34 Drake, A. W., *Fundamentals of Applied Probability Theory*; McGraw Hill Publishing Company, NY, 1988; pp.129-144.
35 Boas, M. *Mathematical Methods in the Physical Sciences*; John Wiley & Sons , NY, 2nd Ed., 1983; pp.685-739.
36 Cashwell, E. D.; Everett, C. J. *A Practical Manual on the Monte Carlo Method for Random Walk Problems*; Pergamon Press, NY, 1959; pp.4-10.
37 Spendley, W.; Hext, G.R.; Himsworth, F.R. *Technometrics* **1962**, 4.4, pp.441-461.
38 Nelder, J.A.; Mead R. *Comp. J* **1964**, pp.308-313.
39 Merck Index, 11th edition, **1989**, pp.1334.
40 Langer, R.; Folkman, J. *Nature* **1976**, 263:5580, pp.797-800.
41 Saltzman, W.M., Langer, R. *Biophys. J.* **1989**, 55, pp.163-171.
42 Siegel, R.; Kost, J.; Langer R. *J. Contr. Rel.* **1989**, 8, pp.223-236.
43 Arakawa, T.; Kita, Y.; Carpenter, F. *Pharm. Res.* **1991**, 8, pp. 285-291.
44 Edelman, E.R.; Mathiowitz, E.; Langer R.; Klagsbrun, M. *Biomaterials* **1991**, 7:12, pp.6119-6126.
45 Andrianov, A.K.; Cohen, S.; Visscher, K.B.; Payne, L.G.; Allcock, H.R.; Langer R. J. Contr. Rel., **1993**, in press.
46 Preis I., Langer R., A single-step immunization by sustained antigen release. *J. Immunol. Methods* 28(1979), p.193-197.
47 Kohn, J.; Niemi, S. M.; Albert, E. C.; Murphy, J. C.; Langer R.; Fox, J. *J. Immunol. Methods* **1986**, 95, 31-38.
48 O'Hagan, D.T.; Rahman, D.; McGee, J.P.; Jeffery, H.; Davies, M.C.; Williams, P.; Davis, S.S.; Challacombe S. *J.Immunology* **1991**, 73, pp. 239-242.
49 Singh, M.; Singh, A.; Talwar, G.P. *Pharm. Res.* **1991**, 8, pp.958-961.
50 Eldridge, J.H.; Staas, J.K.; Meulbroek, J.A.; Tice, T.R.; Gilley, R.M. *Infection and Immunity* **1991**, 59, pp.2978-2986.

51 Alonso, M.J.; Cohen, S.; Park, T.G.; Gupta, R.K.; Siber, G.R.; Langer, R. *Pharm. Res.* **1993**, 51, pp. 945-953.
52 Vranken, M.N.; Claeys, D.A. *U.S. Patent 3,523,906,* 1970.
53 Ogawa, Y.; Yamamoto, M.; Okada, H.; Yashiki, Y.; Shimamoto, T. *Chem. Pharm. Bull.* **1988**, 36, pp.1095-1103.
54 Cohen, S.; Yoshioka, T.; Lucarelli, M.; Hwang, L.H.; Langer R. *Pharm. Res.* **1991**, 8, pp.713-720.
55 Liu, W.R.; Langer, R.; Klibanov, A. *Biotech. Bioeng.* **1991**, 37, pp.177-184.
56 Alonso, M.J.; Gupta, R.K.; Min C.; Siber, G.R.; Langer R. *Vaccine* **1993**, in press.
57 Sluzky, V.; Klibanov, A.M.; Langer R. *Biotech. Bioeng.* **1992**, 40, pp.895-903.
58 Lewis D.H. In: *Biodegradable Polymers as Drug Delivery Systems*, Chasin, M.; Langer, R. Eds., Drugs and the Pharmaceutical Sciences, Marcel Dekker, NY, 1990; Vol. 45, pp.1-41.
59 Esparza, I.; Kissel, T. *Vaccine* **1992**, 10, pp.714-720.
60 Relyveld, E. H.; Mayer, M.M. *Kabat and Mayer's Experimental Immunochemistry*; Thomas, C.C., Ed., Springfield, 1961, pp.22-96.
61 Gupta, R.K.; Maheshwari S.C.; Singh H. *J. Biol. Stand.* **1985**, 13, pp.143-149.
62 Bizzini, B. In: *Bacterial vaccines*; Germanier, R., Ed.; Academic Press, Orlando, 1984, pp. 37-68.
63 Langer, R.; Linhardt, R.; Klein, M.; Flanagan, M.; Galliher, P.; Cooney C. In: *Biomaterials: Interfacial Phenomena and Applications;* Peppas, N.A.; Hoffman, A.; Rather, B.; Cooper, S., Eds.; Advances in Chemistry Series; Washington, D. C., 1982, pp.493-502.
64 Macleod, R. M.; Dunn, F. *J. Acoust. Soc. Am.* **1968**, 44, pp.932-945.
65 Wang, Y.J.; Hanson, M.A. *J. Parent. Sci. Tech.* **1988**, 42(2s), pp.3-26.
66 Tabata, Y.; Langer R. *Pharm. Res.* **1993**, 10.4, pp.487-496.
67 Donbrow, M. *Microcapsules and Nanoparticles in Medicine and Pharmacy*, CRC Press, Boca Raton, Ann Arbor, London, 1992.
68 Müller, R.H. *Colloidal Carriers for Controlled Drug Delivery and Targeting*; CRC Press, Boca Raton, 1991.
69 Davis, S.S; Illum, L., In: *Site-specific Drug Delivery*; E. Tomlinson, E.; Davis, S.S., Eds.; John Willey & Sons, Chichester, 1986, pp. 93.
70 Illum, L.; Davis, S.S. *FEBS Lett.* **1984**, 167, p.79.
71 Allen, T.M.; Hansen, C. *Biochim. Biophys. Acta* **1991**, 1068, 133-141.
72 Allen, T.M.; Hansen, C.; Martin, F.; Redeman, C.; Yau-Young, A. *Biochim. Biophys. Acta* **1991**, 1066, pp.29-36.
73 Torchilin, V.P.; Klibanov, A.L.; Huang, L.; O'Donnel, S.; Nossiff, C.; Khaw, B.A. *FASEB J.* **1992**, 6, pp. 2716-2719.
74 Maruyama, K.; Yuda, T.; Okamoto, A.; Ishikura, C.; Kojima, S.; Iwatsuru, M. *Chem. Pharm. Bull.* **1991**, 39(6), pp.1620-1622.

75 Woodle, M.C.; Matthay, K.K; Hidayat, J.E.; Collins, L.R.; Redemann, C.; Martin, F.J.; Papahadjopoulos, D. *Biochim. Biophys. Acta* **1992**, pp.193-200.
76 Lasic, D.D.; Martin, F.J.; Gabizon, A.; Huang, S.K.; Papahadjopoulos, D.; *BBiochim. Biophys. Acta* **1991**, 1070, pp.187-192.
77 Klibanov, A.; Maruyama, K.; Beckerleg, A.M.; Torchilin, V.P.; Huang, L. *Biochim. Biophys. Acta* **1991**, 1062, pp. 142-148.
78 Gref, R.; Minamitake, Y.; Peraccia, M.T.; Trubetskoy V.; Milshteyn A.; Sinkule, J.; Torchillin, V.; Langer, R. *Proc. Intern. Sympos. Control. Rel. Bioact. Mater.* **1993**, 20, in press.
79 Gref, R.; Minamitake, Y.; Peraccia, M.T.; Langer R. *Macromolecules*, **1993**, pp. 131-132.
80 Zhu, J.E.; Lin, X.; Yang, S.; *J. Polym. Sci., Polym. Lett. Ed.* **1986**, 24, p.331.
81 Brindley, A.;Davies, M.C.; Lynn, R.A.P.; Davis, S.S.; Hearn, J.; Watts, J.F.; *Polymer* **1992**, 33.5, pp. 1112-1115.
82 Miller, D.R.; Peppas, N.A. *J. Macromol. Sci.-Rev. Macromol. Chem. Phys.* **1986**, C26(1), pp.33-66.
83 Torchilin, V.; Klibanov, A. *Critical Reviews in Therapeutic Drug Carrier Systems* **1991**, 7.4, pp. 275-307.

RECEIVED April 19, 1994